Shared-Sensing and Control Using Reversible Transducers

Tuhin Das and Ranjan Mukherjee

***Abstract*—As an alternative to self-sensing, we propose the concept of shared-sensing for reversible transducers. In shared-sensing, reversible transducers are continuously switched between actuator and sensor modes. This results in a hybrid system, and, in this paper, we investigate stability properties of the equilibrium for linear systems and a class of nonlinear systems with a single shared-sensing transducer. Our theoretical results are validated through simulations and experiments with a dc servo motor.**

***Index Terms*—DC motors, piezoelectric transducers, reversible transducer, self-sensing, shared-sensing, stability, ultimate boundedness.**

I. Introduction

MANY transducers are reversible in nature and can be used both as sensors and actuators. Examples are electric motors, piezoelectric devices, and thermocouples. Reversible properties of transducers have been exploited by researchers by implementing self-sensing schemes, wherein the transducers are simultaneously used as sensors and actuators. Self-sensing has been attempted in several applications, but its limitations are known and documented in the literature. For example, self-sensing magnetic bearings lack robustness [12], and self-sensing piezoelectrics are sensitive to error in estimation of transucer capacitance [2], [6], [10].

In shared-sensing, sensing and actuation are performed alternately and the goal of this paper is to explore shared-sensing with the objective of developing a general framework for observer based control design. In Section II-A, we discuss the switched system resulting from shared-sensing, and, in Section II-B, we investigate stabilization of open-loop-stable linear systems. Simulation and experimental results of shared-sensing in an open-loop stable linear system can be found in [11] and are not presented here. In Section II-C, we consider stabilization of open-loop-unstable linear systems. As an example, we consider stabilization of the inverted pendulum using a dc servo motor operating in shared-sensing mode. In the absence of a joint angle sensor, actuation of the motor is periodically disabled and the back-EMF is sensed to estimate the joint angle. Existing approaches to sensorless motor control are based on back-EMF measurement, flux-linkage calculation, current detection in free-wheeling diodes, and speed-independent flux linkage function calculation, to name a few [8]. The common drawback of these techniques is the inaccuracy of position estimation at low speeds and results in the literature indicate that self-sensing can be used for velocity tracking but cannot provide satisfactory position control [1]. Using shared-sensing, we accomplish position control by balancing the pendulum in its vertically upright unstable position. Simulation results of this system are presented in Section III-A, and experimental results are provided in Section IV-A. Linearization has the effect of a nominal input being applied to the system which cannot be compensated during sensing and can result in steady-state errors. Using a feedforward term during actuation, we show that trajectories are ultimately bounded and the ultimate bound is proportional to the switching interval. Simulation results for an example system are presented in Section III-B, and experimental results are provided in Section IV-B. Section V contains concluding remarks.

Manuscript received September 13, 2007; revised March 04, 2008. Manuscript received in final form April 03, 2008. First published June 13, 2008; current version published December 24, 2008. Recommended by Associate Editor A. Giua. This work was supported by the National Science Foundation under NSF Grant CMS-0409388.

T. Das is with the Department of Mechanical Engineering, Rochester Institute of Technology, Rochester, NY 14623 USA (e-mail: tkdeme@rit.edu).

R. Mukherjee is with the Department of Mechanical Engineering, Michigan State University, East Lansing, MI 48824-1226 USA (e-mail: mukherji@egr.msu.edu)

Digital Object Identifier 10.1109/TCST.2008.924570

II. Observer-Based Control Using Reversible Transducers

A. Switched System Description

Consider a linear system with a single reversible transducer. Let the system be completely controllable when the transducer is in the actuator mode and completely observable when the transducer is in the sensor mode. Let the time period of switching be equal to δ and let n and $(1-n)$ be the fractions of time in the actuator mode and sensor mode, respectively. When the transducer is in the actuator mode, the system has the state space description

$$\begin{aligned}&\dot{x} = Ax + Bu\\ &y = [0], \quad t_0 + k\delta \le t < t_0 + (k+n)\delta, \quad k = 0,1,2,\ldots\end{aligned} \tag{1}$$

In the sensor mode, the system has the state space description

$$\begin{aligned}&\dot{x} = Ax\\ &y = Cx, \quad t_0 + (k+n)\delta \le t < t_0 + (k+1)\delta,\\ &\qquad k = 0,1,2,\ldots\end{aligned} \tag{2}$$

For the switched system described by (1) and (2), we design a state estimator as follows:

$$\dot{\hat{x}} = \begin{cases} A\hat{x} + Bu, & t_0 + k\delta \le t < t_0 + (k+n)\delta\\ A\hat{x} + L(y - \hat{y}), & t_0 + (k+n)\delta \le t < t_0 + (k+1)\delta\\ & k = 0,1,2,\cdots \end{cases} \tag{3}$$

where $\hat{x}$ denotes the estimated states and L denotes the estimator gains. With the input of the form $u = -K\hat{x}$, where K denotes the controller gains, the complete system can be described as

$$\dot{X} = \begin{cases} A_1 X, & t_0 + k\delta \le t < t_0 + (k+n)\delta\\ A_2 X, & t_0 + (k+n)\delta \le t < t_0 + (k+1)\delta\\ & k = 0,1,2,\cdots \end{cases} \tag{4}$$

where

$$X = \begin{bmatrix} x \\ \tilde{x} \end{bmatrix}, \quad \tilde{x} = (x - \hat{x}) \tag{5}$$

$$A_1 = \begin{bmatrix} A - BK & BK \\ 0 & A \end{bmatrix}$$

$$A_2 = \begin{bmatrix} A & 0 \\ 0 & A - LC \end{bmatrix}. \tag{6}$$

Since A_1 and A_2 are block triangular, the eigenvalues of A_1 are those of $(A - BK)$ and A, and eigenvalues of A_2 are those of A and $(A - LC)$.

B. Open-Loop-Stable Linear Systems

Since A is Hurwitz and $(A - BK)$ and $(A - LC)$ can be made Hurwitz through proper choice of K and L matrices, respectively, A_1 and A_2 in (4) can be designed to be Hurwitz. Consequently, asymptotic stability of the switched system in (4) can be guaranteed by ensuring slow-switching on-the-average [5] or simply using switching intervals greater than the "*dwell time*" [9].

C. Open-Loop-Unstable Linear Systems

From (4), we can write

$$X(t_{j+2}) = e^{A_2(1-n)\delta} e^{A_1 n\delta} X(t_j), \quad j = 0, 2, 4, \ldots \tag{7}$$

We next define a linear system that is "*equivalent*" to the switched system.

Definition 1—Discrete Equivalent (DE): The time-invariant linear system

$$\dot{X} = A_{\text{eq}} X \tag{8}$$

is a DE of a switched linear system if the state variables of the two systems assume identical values at regular intervals of time, after starting from the same initial condition. Based on the above definition, $\dot{X} = A_{\text{eq}} X$, is a DE of the switched system in (4) with

$$A_{\text{eq}} = \frac{1}{\delta} \ln[e^{A_2(1-n)\delta} e^{A_1 n\delta}]. \tag{9}$$

Since A_{eq} is the logarithm of a matrix, the issues of existence and uniqueness of A_{eq} arises. We address these issues after we present the condition for stability of the switched system.

Theorem 1—Exponential Stability: The origin of the switched system described by (4) is exponentially stable if A_{eq} of the DE system in (9) is Hurwitz.

Proof: For the DE system, assume $\| X(t_0) \| = \epsilon$. Since A_{eq} is Hurwitz, we have

$$\begin{aligned} X(t) &= e^{A_{\text{eq}}(t-t_0)} X(t_0) \\ \Longrightarrow \| X(t) \| &\leq \| e^{A_{\text{eq}}(t-t_0)} \| \| X(t_0) \| \\ &\leq \gamma e^{-\lambda(t-t_0)} \epsilon \end{aligned} \tag{10}$$

where $\gamma, \lambda > 0$ are positive numbers. Since the states of the switched system and its DE assume identical values at $t = t_0 + k\delta$, $k = 0, 1, 2, \cdots$, the states of the switched system satisfy

$$\begin{aligned} \| X(t_0 + m\delta) \| &\leq \gamma \epsilon e^{-\lambda m\delta} \\ \| X[t_0 + (m+1)\delta] \| &\leq \gamma \epsilon e^{-\lambda(m+1)\delta} \end{aligned} \tag{11}$$

for any positive integer value of m. Now consider the time interval $t_0 + m\delta \leq t \leq t_0 + (m+1)\delta$. Within this interval, first consider the actuation subinterval $(t_0 + m\delta) \leq t \leq (t_0 + m\delta + n\delta)$. Using (11) and the relation $(m\delta + \tau_1) = (t - t_0)$, we have

$$\begin{aligned} X(t_0 + m\delta + \tau_1) &= e^{A_1 \tau_1} X(t_0 + m\delta) \\ \Longrightarrow \| X(t_0 + m\delta + \tau_1) \| &\leq \| e^{A_1 \tau_1} \| \| X(t_0 + m\delta) \| \\ &\leq e^{\eta_1 \tau_1} \gamma \epsilon e^{-\lambda m\delta} \\ &\leq \gamma \epsilon e^{(\eta_1 + \lambda)\tau_1} e^{-\lambda(m\delta + \tau_1)} \\ \Longrightarrow \| X(t) \| &\leq \gamma \epsilon e^{(\eta_1 + \lambda) n\delta} e^{-\lambda(t - t_0)} \end{aligned} \tag{12}$$

where $0 \leq \tau_1 \leq n\delta$ and $\eta_1 = \| A_1 \|$. Similarly, for the sensing subinterval $[t_0 + (m+1)\delta - (1-n)\delta] \leq t \leq [t_0 + (m+1)\delta]$, we can use the expressions $0 \leq \tau_2 \leq (1-n)\delta$, $[(m+1)\delta - \tau_2] = (t - t_0)$, and $\eta_2 = \| A_2 \|$, to show

$$\begin{aligned} X[t_0 + (m+1)\delta - \tau_2] &= e^{-A_2 \tau_2} X[t_0 + (m+1)\delta] \\ \Longrightarrow \| X(t) \| &\leq \gamma \epsilon e^{|\eta_2 - \lambda|(1-n)\delta} e^{-\lambda(t - t_0)}. \end{aligned} \tag{13}$$

From (12) and (13), we deduce

$$\begin{aligned} \| X(t) \| &\leq \gamma \, \epsilon \, \kappa_1 e^{-\lambda(t - t_0)} \\ \kappa_1 &\equiv \max[e^{(\eta_1 + \lambda) n\delta}, e^{|\eta_2 - \lambda|(1-n)\delta}] \end{aligned} \tag{14}$$

which implies exponential stability of $X = 0$ for the switched system. ◇◇◇

Remark 1: A necessary and sufficient condition for existence of A_{eq} in (9) is that the matrix $M \triangleq e^{A_2(1-n)\delta} e^{A_1 n\delta}$ is nonsingular [3]. From the structures of A_1 and A_2 in (6), we can show that the eigenvalues of M are those of the submatrices $e^{A(1-n)\delta} e^{(A - BK)n\delta}$ and $e^{(A-LC)(1-n)\delta} e^{An\delta}$. The submatrices can be made nonsingular through proper choice of K and L matrices and therefore the existence of A_{eq} can be guaranteed through proper choice of controller and observer gains. The uniqueness of A_{eq} is not an issue since all solutions of A_{eq} obtained from (9) will have the same eigenvalues [3], and the results of Theorem 1 are based on the Hurwitz property of A_{eq} and not on the entries of A_{eq}. This also implies that the DE of a switched linear system may not be unique.

D. Linearized Systems

We consider nonlinear systems with a single transducer of the form

$$\dot{z} = p(z) + B\nu, \quad w = h(z) \tag{15}$$

where z is the state vector, ν is the single control input in actuator mode, and w is the single output in sensor mode. The

functions $p(z)$ and $h(z)$ are assumed to be Lipschitz in z for $z \in \mathcal{B} = \{z \in R^r | \parallel z - z_0 \parallel \leq d\}$, with Lipschitz constants L_1 and L_2, respectively, where z_0 is the operating point. In the actuator mode, linearization about $(z, \nu) = (z_0, \nu_0)$ results in

$$\begin{aligned} \dot{x} &= Ax + Bu \\ y &= 0, \quad t_0 + k\delta \leq t < t_0 + (k+n)\delta \end{aligned} \tag{16}$$

where $x = (z - z_0)$, $u = (\nu - \nu_0)$

$$A = \left.\frac{\partial f}{\partial z}\right|_{z=z_0} \tag{17}$$

and ν_0 is chosen such that $p(z_0) + B\nu_0 = 0$. In the sensor mode, the system equations are

$$\begin{aligned} \dot{x} &= Ax + F \\ y &= Cx, \qquad t_0 + (k+n)\delta \leq t < t_0 + (k+1)\delta \end{aligned} \tag{18}$$

where

$$F = f(z_0, 0) \tag{19}$$

and $y = Cx$ represents the linearized output equation where

$$y = (w - w_0) \quad w_0 = h(z_0) \quad C = \left.\frac{\partial h}{\partial z}\right|_{z=z_0}. \tag{20}$$

For the switched system described by (16) and (18), we design the state estimator

$$\dot{\hat{x}} = \begin{cases} A\hat{x} + Bu, & t_0 + k\delta \leq t < t_0 + (k+n)\delta \\ A\hat{x} + F + L(y - \hat{y}), & t_0 + (k+n)\delta \leq t < t_0 + (k+1)\delta \end{cases} \tag{21}$$

The control input is designed as $u = -K\hat{x} + u_d$, where u_d is a constant that will be chosen to mitigate the effect of F. The complete system can be described as

$$\dot{X} = \begin{cases} A_1 X + B^* u_d, & t_0 + k\delta \leq t < t_0 + (k+n)\delta \\ A_2 X + F^*, & t_0 + (k+n)\delta \leq t < t_0 + (k+1)\delta \end{cases} \tag{22}$$

where

$$B^* = \begin{bmatrix} B \\ 0 \end{bmatrix} \qquad F^* = \begin{bmatrix} F \\ 0 \end{bmatrix}. \tag{23}$$

From (22), we can write

$$\begin{aligned} X[t_0 + (k+1)\delta] = e^{A_2(1-n)\delta} e^{A_1 n\delta} X(t_0 + k\delta) \\ + n\delta B^* u_d + (1-n)\delta F^* + \kappa_2 \delta^2 \end{aligned} \tag{24}$$

where κ_2 is a constant whose value depends on n, δ, A_1, A_2, B^*, F^*, and u_d. We can show that

$$u_d = \left(\frac{1-n}{n}\right)\nu_0 \Longrightarrow n\delta B^* u_d + (1-n)\delta F^* = [0]. \tag{25}$$

Based on the above choice of u_d, the DE of the linearized switched system, described by (22), is

$$\dot{X} = A_{\text{eq}} X + \left[e^{A_{\text{eq}}\delta} - I\right]^{-1} A_{\text{eq}}\, \kappa_2\, \delta^2. \tag{26}$$

We now establish ultimate boundedness of trajectories of the nonlinear system with the help of the next two theorems.

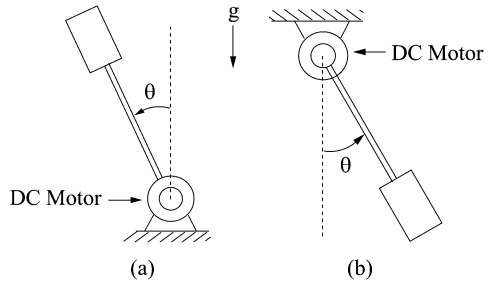

Fig. 1. Pendulum configurations. (a) Inverted. (b) At an acute angle.

Theorem 2: Ultimate Boundedness of Linearized System: The trajectories of the linearized switched system, described by (22), are ultimately bounded if A_{eq} of the DE system in (26) is Hurwitz and u_d is chosen according to (25).

Proof: See the Appendix.

The nonlinear switched system can be written as

$$\begin{aligned} \dot{x}_n &= Ax_n + Bu + g_1(x_n) \\ y &= 0, \qquad\qquad t_0 + k\delta \leq t < t_0 + (k+n)\delta \\ \dot{x}_n &= Ax_n + F + g_1(x_n) \\ y &= Cx_n + g_2(x_n), \qquad t_0 + (k+n)\delta \leq t < t_0 + (k+1)\delta \end{aligned} \tag{27}$$

where x_n are the states and $g_1(x_n)$ and $g_2(x_n)$ have the form

$$\begin{aligned} g_1(x_n) &= p(z) - p(z_0) - Ax_n \\ g_2(x_n) &= h(z) - h(z_0) - Cx_n. \end{aligned} \tag{28}$$

With the observer design in (21) and the control input chosen as $u = -K\hat{x} + u_d$, the closed-loop nonlinear switched system becomes

$$\dot{X}_n = \begin{cases} A_1 X_n + B^* u_d + \bar{g}_1(X_n), \\ \qquad t_0 + k\delta \leq t < t_0 + (k+n)\delta \\ A_2 X_n + F^* + \bar{g}_2(X_n), \\ \qquad t_0 + (k+n)\delta \leq t < t_0 + (k+1)\delta \end{cases} \tag{29}$$

where $X_n = [x_n \tilde{x}_n]^T$, $\tilde{x}_n = (x_n - \hat{x})$, and

$$\begin{aligned} \bar{g}_1(X_n) &= \begin{bmatrix} g_1(x_n) \\ g_1(x_n) \end{bmatrix} \\ \bar{g}_2(X_n) &= \begin{bmatrix} g_1(x_n) \\ g_1(x_n) - L\, g_2(x_n) \end{bmatrix}. \end{aligned} \tag{30}$$

Theorem 3: Ultimate Boundedness of Nonlinear System: The trajectories of the nonlinear switched system described by (29) are ultimately bounded if A_{eq} is Hurwitz and u_d is chosen according to (25).

Proof: See the Appendix.

From the proofs of Theorem 3, it can be seen that the ultimate bound depends on the length of the switching interval δ.

III. Simulations

A. Open-Loop-Unstable Linear Systems

The development in Section II-C is validated through simulation of a pendulum maintained in the inverted configuration by a dc servo motor. A schematic of the system is shown in Fig. 1(a). Corresponding to (1) and (2), the states are $x = [\theta \quad \dot{\theta} \quad i]^T$,

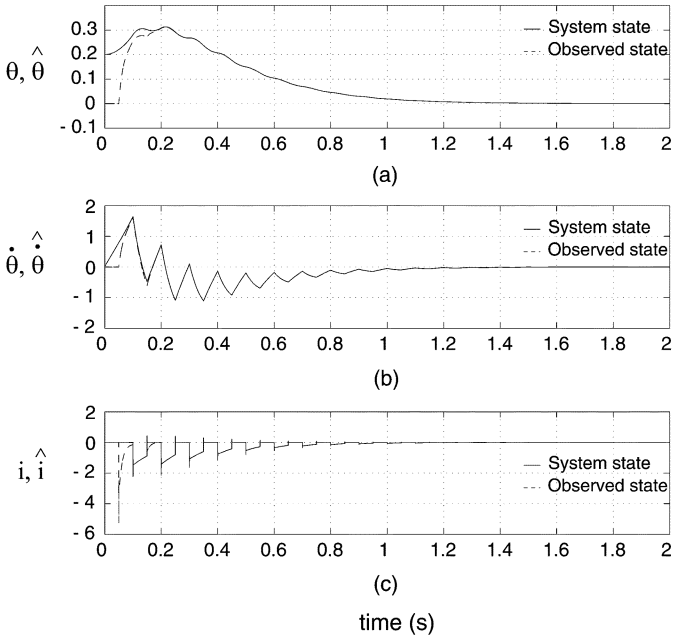

Fig. 2. Inverted pendulum control using a shared-sensing dc motor.

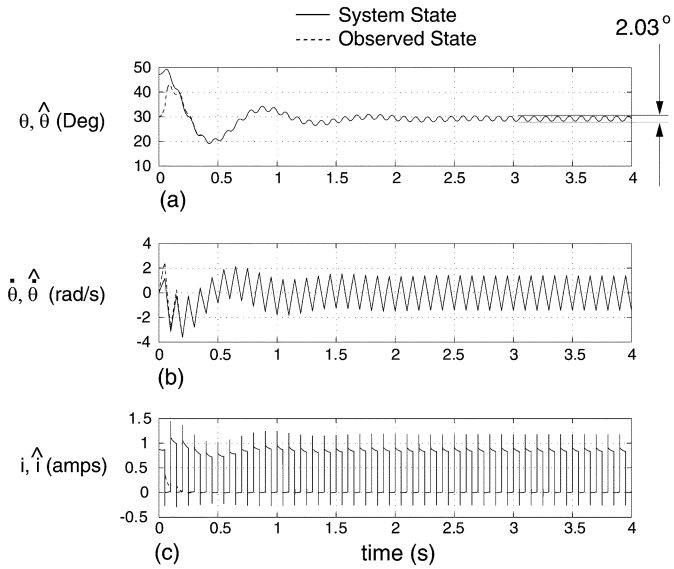

Fig. 3. Shared sensing and control of pendulum at 30° with $n = 0.5$, and $\delta = 0.1$ s.

where i is the motor current. The input u and output y are the control voltage and back-EMF, respectively. The matrices A, B, and C have the form

$$A = \begin{bmatrix} 0 & 1 & 0 \\ \frac{mgL}{I} & -\frac{b}{I} & \frac{K_m}{I} \\ 0 & -\frac{K_m}{L_a} & -\frac{R_a}{L_a} \end{bmatrix}$$
$$B = \begin{bmatrix} 0 \\ 0 \\ \frac{1}{L_a} \end{bmatrix}$$
$$C = [0 \quad K_m \quad 0] \tag{31}$$

where m is the mass of the pendulum, L is its effective length, b is the damping coefficient, and I is the mass moment of inertia about the center of rotation. R_a and L_a denote the resistance and inductance of the motor and K_m represents the motor constant. The values of these parameters, used in simulations, are assumed to be

$$\begin{aligned} mgL &= 0.0677\,\text{kg m}^2/\text{s}^2 \\ I &= 8.327 \times 10^{-4}\,\text{kg m}^2 \\ L_a &= 640 \times 10^{-6}\,\text{H} \\ b &= 0.002\,\text{kg m}^2/\text{s} \\ R_a &= 9.5\Omega \\ K_m &= 0.047\,\text{N} \cdot \text{m/A}. \end{aligned} \tag{32}$$

It can be verified that A is not Hurwitz. For exponential stability, we chose $\delta = 0.1$ s, $n = 0.5$, and K and L matrices such that A_{eq} is Hurwitz. The simulation results are shown in Fig. 2.

The ratio of the $\mathcal{L}_2$ norms of the output and input, which can be viewed as the energy amplification gain, was computed to be 4.04×10^{-3}. Later, it will be compared with the ratio obtained from experimental data. The "worst-case" energy amplification gain, referred to as the rms gain in the literature, has been computed for switched systems with large switching intervals and open-loop stable system descriptions [4].

B. Linearized Systems

We consider the problem of maintaining the pendulum at angle $\theta = \theta_0$, as shown in Fig. 1(b). The dynamics of this system described by (15), where $z = [\theta \quad \dot{\theta} \quad i]^T$, i is the motor current, ν is the control voltage, has the form

$$\dot{z} = \begin{bmatrix} z_2 \\ -\frac{mgL}{I}\sin z_1 - \frac{b}{I}z_2 + \frac{K_m}{I}z_3 \\ -\frac{K_m}{L_a}z_2 - \frac{R_a}{L_a}z_3 + \frac{1}{L_a}\nu \end{bmatrix}. \tag{33}$$

The linearized equations are described by (16) and (18) where A and F have the form

$$A = \begin{bmatrix} 0 & 1 & 0 \\ -\frac{mgL}{I}\cos\theta_0 & -\frac{b}{I} & \frac{K_m}{I} \\ 0 & -\frac{K_m}{L_a} & -\frac{R_a}{L_a} \end{bmatrix}$$
$$F = \begin{bmatrix} 0 \\ 0 \\ -\frac{R_a}{L_a}\frac{mgL}{K_m}\sin\theta_0 \end{bmatrix} \tag{34}$$

and B and C are given in (31). The simulation results for $\delta = 0.1$ s and 0.05 s are shown in Figs. 3 and 4, respectively. For both of these simulations, we chose $\theta_0 = 30°$, $n = 0.5$, and K and L matrices that result in A_{eq} being Hurwitz. In accordance with (25), u_d was chosen as

$$u_d = \left(\frac{1-n}{n}\right) Ra\,\frac{mgL}{K_m}\sin\theta_0 \tag{35}$$

to mitigate the effect of gravity. It is clear from Figs. 3 and 4 that the state variable trajectories are ultimately bounded. Furthermore, the ultimate bound is smaller for a smaller value of δ.

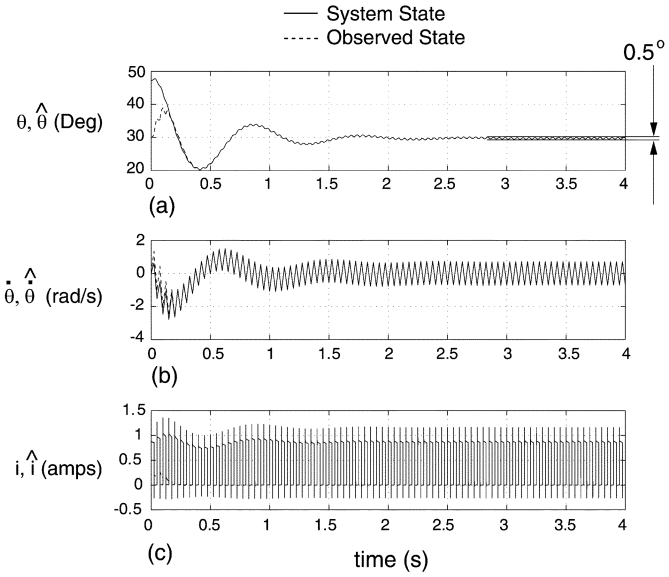

Fig. 4. Shared sensing and control of pendulum at 30° with $n = 0.5$, and $\delta = 0.05$ s.

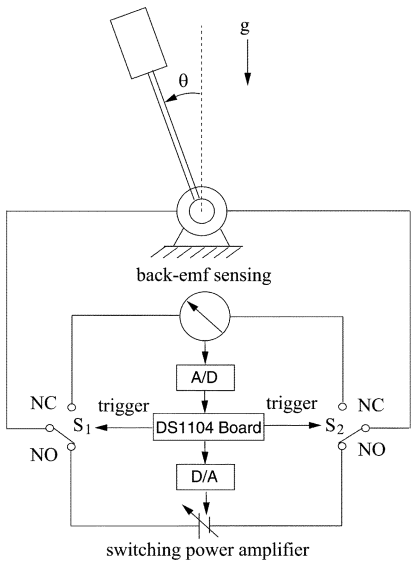

Fig. 5. Shared-sensing and control setup for inverted pendulum.

IV. Experiments

A. Open-Loop-Unstable Linear Systems

The experimental setup is shown schematically in Fig. 5. S_1 and S_2 are mechanical single pole double throw (SPDT) relays which are simultaneously switched to the NO (Normally Open) position in the actuation mode and to the NC (Normally Closed) position in the sensing mode. The system parameters are the same as those used in Section III-A and are given in (32). The logic signals for the relays and the observer-based controller were programmed in MATLAB/Simulink and executed using a dSpace DS 1104 real-time controller.

As in our simulations in Section III-A, we used $\delta = 0.1$s and $n = 0.5$. The angle of the pendulum, relative to the vertically down position, α, was measured by an encoder. The estimated angular position of the pendulum $\hat{\theta}$ was measured relative to

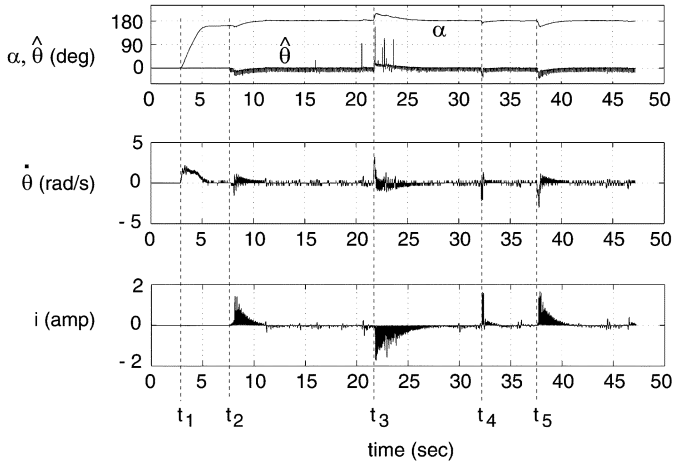

Fig. 6. Measured and observed variables of inverted pendulum.

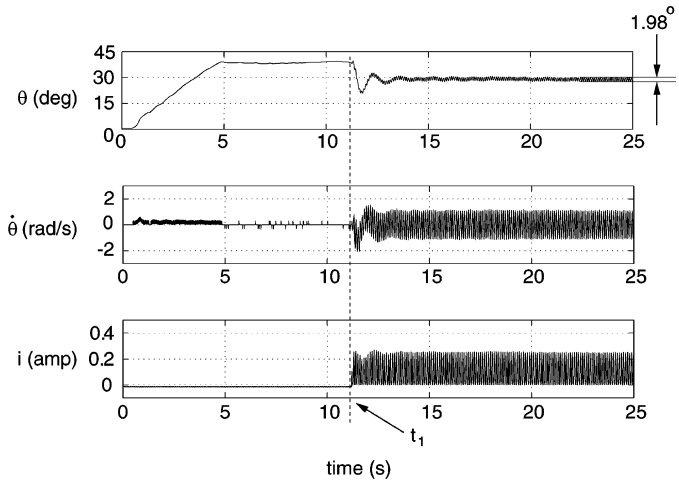

Fig. 7. Ultimate boundedness of pendulum angle about $\theta = 30°$ for $\delta = 0.1$ s and $n = 0.5$.

the vertically upright position. The plot of these and other state variables are shown in Fig. 6. Initially, the pendulum was in the vertically down position. It was manually taken to $\alpha \approx 160°$ over the time interval $t_1 - t_2$ and released. At time t_2, the observer based controller was invoked to stabilize the top equilibrium configuration of the pendulum. The initial value of the observer state, $\hat{\theta}$, was assumed to be zero and this explains the zero value of $\hat{\theta}$ over the interval $t = 0$ to $t = t_2$. The pendulum was perturbed by upto 20° at times t_3, t_4, and t_5, and the plots in Fig. 6 confirm asymptotic stability property of the equilibrium. Over the interval $t_2 - t_3$, the energy amplification gain was computed to be 4.3×10^{-3}. This value matches closely with that obtained from simulations in Section III-A.

B. Linearized Systems

We validate the simulation result of Section III-B corresponding to $\delta = 0.1$ s and $n = 0.5$. We use the experimental hardware that is described in Section IV-A and whose parameters are tabulated in Section III-A. The definition of angle θ is, however, in accordance with Fig. 1(b). The experimental results are shown in Fig. 7. Over the interval $t_0 - t_1$, the pendulum was manually taken to $\theta \approx 40°$. At t_1, the pendulum was released

and the observer-based controller of Section II-D was invoked. The results indicate that the trajectories of the pendulum are ultimately bounded about the operating point $\theta = 30^\circ$. The amplitude of oscillation of the pendulum is approximately 2° and this matches closely with the simulation results in Fig. 3.

V. Conclusion

We proposed the concept of shared-sensing in reversible transducers. In contrast to self-sensing, where sensing and actuation are simultaneously performed, shared-sensing is realized by periodically switching between sensing and actuation modes. We designed observer based controllers for open-loop-stable and open-loop-unstable linear systems and a class of nonlinear systems. For open-loop-unstable linear systems, we demonstrated shared-sensing by balancing an inverted pendulum using an electric motor. The experimental results are promising in light of the fact that self-sensing in electric motors fails to accurately estimate rotor position at low speeds. The systems obtained through linearization result in a constant disturbance input and shared-sensing can guarantee ultimate boundedness of trajectories. Using simulations and experiments, we demonstrated ultimate boundedness of the pendulum angle around a non-zero operating point. The theoretical development in this paper assumed a single transducer and our future work will address the problem of optimal partitioning of multiple transducers between actuator and sensor modes.

Appendix
Proof of Theorem 2

Since $A_{\rm eq}$ is Hurwitz, from (26), we can write

$$\begin{aligned}\lim_{k\to\infty} X(t_0+k\delta) &= \lim_{k\to\infty} X[t_0+(k+1)\delta] \\ &= -[e^{A_{\rm eq}\delta}-I]^{-1}\,\kappa\,\delta^2. \end{aligned} \tag{36}$$

Consider the time interval $t_0+k\delta \le t \le t_0+(k+1)\delta$. Within this interval, consider the actuation subinterval $(t_0+k\delta) \le t \le (t_0+k\delta+n\delta)$. From (22), (25), and (36), we get

$$\begin{aligned} X(t_0+k\delta+\tau_1) &= -e^{A_1\tau_1}[e^{A_{\rm eq}\delta}-I]^{-1}\,\kappa\,\delta^2 \\ &\quad + \int_0^{\tau_1} e^{A_1\sigma}B^*u_d\,d\sigma \\ &= -e^{A_1\tau_1}[e^{A_{\rm eq}\delta}-I]^{-1}\,\kappa\,\delta^2 \\ &\quad + A_1^{-1}[e^{A_1\tau_1}-I]B^*u_d \\ \Rightarrow \|X(t_0+k\delta+\tau_1)\| &\le e^{\|A_1\|\tau_1}\|[e^{A_{\rm eq}\delta}-I]^{-1}\|\,\|\kappa\|\delta^2 \\ &\quad + \|A_1^{-1}\|[e^{\|A_1\|\tau_1}-1]\|B^*u_d\| \\ \Rightarrow \|X(t)\| &\le e^{\eta_1 n\delta}\eta_3\,\|\kappa\|\,\delta^2 \\ &\quad + \zeta_1[e^{\eta_1 n\delta}-1]\|F^*\|(1-n) \triangleq \rho_1 \\ &= e^{\eta_1 n\delta}\eta_3\;\|\,\kappa\,\|\;\delta^2 \\ &\quad + \zeta_1\eta_1 n\left[1+\frac{\eta_1 n\delta}{2!}+\frac{\eta_1^2 n^2\delta^2}{3!}+\cdots\right] \\ &\quad \times \|F^*\|\,(1-n)\,\delta \end{aligned} \tag{37}$$

where $0 \le \tau_1 < n\delta$, $\eta_1 = \|A_1\|$, $\zeta_1 = \|A_1^{-1}\|$, $\eta_{\rm eq} = \|A_{\rm eq}\|$, $\eta_3 = \|(e^{A_{\rm eq}\delta}-I)^{-1}\|$. A_1 and $(e^{A_{\rm eq}\delta}-I)$ are invertible $r\times r$ matrices. For the sensing subinterval $[t_0+(k+1)\delta-(1-n)\delta] \le t \le [t_0+(k+1)\delta]$, we can use (22), and (36) to show

$$\begin{aligned} \|X(t)\| &\le e^{\eta_2(1-n)\delta}\eta_3\|\kappa\|\delta^2 + \zeta_2[e^{\eta_2(1-n)\delta}-1]\|F^*\| \\ &\triangleq \rho_2 \\ &= e^{\eta_2(1-n)\delta}\eta_3\|\kappa\|\delta^2 + \zeta_2\eta_2(1-n) \\ &\quad \times\left[1+\frac{\eta_2(1-n)\delta}{2!}+\frac{\eta_2^2(1-n)^2\delta^2}{3!}+\cdots\right] \\ &\quad \times \|F^*\|\delta \end{aligned} \tag{38}$$

where $0 \le \tau_2 \le (1-n)\delta$, $\eta_2 = \|A_2\|$, $\zeta_2 = \|A_2^{-1}\|$, and A_2 is an invertible $r\times r$ matrix. From (37) and (38), we deduce that the states of the linearized switched system is ultimately bounded with ultimate bound $\beta = \max[\rho_1,\rho_2]$. Since ρ_1 and ρ_2 are increasing functions of δ, the ultimate bound β will be small for small values of δ and *vice versa*. $\diamond\diamond\diamond$

Proof of Theorem 3: The difference between the nonlinear and linearized switched system is studied by constructing the state equation

$$\dot{E} = \begin{cases} A_1E+\bar{g}_1(X_n), \\ \quad t_0+k\delta \le t < t_0+(k+n)\delta \\ A_2E+\bar{g}_2(X_n), \\ \quad t_0+(k+n)\delta \le t < t_0+(k+1)\delta \end{cases} \tag{39}$$

where $E = (X_n - X)$. Hence

$$\begin{aligned} &E(t_0+(k+1)\delta) \\ &\quad = e^{A_2(1-n)\delta}e^{A_1 n\delta}E(t_0+k\delta) \\ &\qquad + e^{A_2(1-n)\delta}\int_{t_0+k\delta}^{t_0+(k+n)\delta} e^{A_1(t_0+(k+n)\delta-\tau)}\bar{g}_1(X_n)d\tau \\ &\qquad + \int_{t_0+(k+n)\delta}^{t_0+(k+1)\delta} e^{A_2(t_0+(k+1)\delta-\tau)}\bar{g}_2(X_n)d\tau. \end{aligned} \tag{40}$$

Considering the time-instant $t = t_0+k\delta, k = 1,2,\cdots\infty$, a DE of the system in (39) is

$$\dot{E} = A_{\rm eq}E + q(t) \tag{41}$$

where $q(t) = q_k$ is a constant for $t_0+k\delta \le t < t_0+(k+1)\delta$. From (41), we have

$$\begin{aligned} E(t_0+(k+1)\delta) &= e^{A_{\rm eq}\delta}E(t_0+k\delta) \\ &\quad + \int_{t_0+k\delta}^{t_0+(k+1)\delta} e^{A_{\rm eq}(t_0+(k+1)\delta-\tau)}d\tau\,q_k. \end{aligned} \tag{42}$$

By comparing (40) and (42), we get

$$q_k = (e^{A_{\rm eq}\delta} - I)^{-1} A_{\rm eq} \times \left(e^{A_2(1-n)\delta} \int_{t_0+k\delta}^{t_0+(k+n)\delta} e^{A_1(t_0+(k+n)\delta-\tau)} \bar{g}_1(X_n) d\tau + \int_{t_0+(k+n)\delta}^{t_0+(k+1)\delta} e^{A_2(t_0+(k+1)\delta-\tau)} \bar{g}_2(X_n) d\tau \right). \quad (43)$$

Since $A_{\rm eq}$ is Hurwitz, $(e^{A_{\rm eq}\delta} - I)$ is invertible. From (43), we can show

$$\|q_k\| \le q_{\rm mod}\,\delta \parallel X_n \parallel$$
$$q_{\rm mod} \triangleq \eta_3\eta_{\rm eq} e^{\eta_2(1-n)\delta}\left(e^{\eta_1 n\delta}\mu_1 n + \mu_2(1-n)\right) \quad (44)$$

where η_1, η_2, η_3, and $\eta_{\rm eq}$ were defined in the proof of Theorem 2, $\parallel \bar{g}_1(X_n) \parallel \le \mu_1 \parallel X_n \parallel$, and $\parallel \bar{g}_2(X_n) \parallel \le \mu_2 \parallel X_n \parallel$. The expressions for μ_1 and μ_2 are derived from (28) using Lipschitz constants L_1 and L_2 as follows:

$$\begin{aligned} \parallel g_1(x_n) \parallel &\le \parallel p(z) - p(z_0) \parallel + \parallel A \parallel\parallel x_n \parallel \\ &\le L_1 \parallel z - z_0 \parallel + \parallel A \parallel\parallel x_n \parallel \\ &\le (L_1 + \parallel A \parallel) \parallel X_n(t) \parallel \quad (45) \\ \parallel g_2(x_n) \parallel &\le (L_2 + \parallel C \parallel) \parallel X_n(t) \parallel . \quad (46) \end{aligned}$$

From the definitions of $\bar{g}_1$ and $\bar{g}_2$ in (30), we can show using the Holder Inequality that

$$\mu_1 = \sqrt{2}\,(L_1 + \parallel A \parallel)$$
$$\mu_2 = \sqrt{3(L_1 + \parallel A \parallel)^2 + 2\parallel L \parallel^2 (L_2 + \parallel C \parallel)^2}. \quad (47)$$

Using (44), we rewrite (41) as follows:

$$\dot{E} \le A_{\rm eq}E + q_{\max}, \quad q_{\max} = q_{\rm mod}\,\delta M \parallel X_n(t) \parallel \quad (48)$$

where, $M = (1/\sqrt{r})[11\cdots 1]^T$ is an $r \times 1$ vector. Using the Comparison Lemma [7], the following ultimate bound of the DE system is deduced:

$$\parallel E \parallel \le q_{\rm mod}\,\delta \parallel A_{\rm eq}^{-1} \parallel\parallel X_n \parallel \quad (49)$$

Since the DE system states are identical to the states of the switched system at $t = t_0 + k\delta, k = 1, 2, \cdots \infty$, for the switched system in (39), we claim, for $k \to \infty$, that

$$\begin{aligned} \parallel E(t_0 + k\delta) \parallel &\le q_{\rm mod}\,\delta \parallel A_{\rm eq}^{-1} \parallel\parallel X_n \parallel \\ &\le q_{\rm mod}\,\delta\eta_4 \parallel X_n \parallel \quad (50) \end{aligned}$$

where $\eta_4 = \parallel A_{\rm eq}^{-1} \parallel$. To obtain the ultimate bound for all t over the interval $t_0 + k\delta \le t \le t_0 + (k+1)\delta$, where $k \to \infty$, consider the actuation subinterval $(t_0 + k\delta) \le t \le (t_0 + k\delta + n\delta)$. Using (39), (44), (47) and (50), we can write

$$E(t_0 + k\delta + \tau_1) = e^{A_1\tau_1}E(t_0 + k\delta) + \int_0^{\tau_1} e^{A_1(\xi)}\bar{g}_1(X_n)d\xi$$
$$\Rightarrow \parallel E(t) \parallel \le\ e^{\eta_1 n\delta}(\eta_4 q_{\rm mod} + n\mu_1)\delta \parallel X_n(t) \parallel \quad (51)$$

where, $0 \le \tau_1 < n\delta$. For the sensing subinterval $(t_0 + k\delta + n\delta) \le t \le (t_0 + (k+1)\delta)$ we obtain using (39), (44), (47) and (50)

$$E(t_0 + (k+1)\delta - \tau_2) = e^{-A_2\tau_2}E(t_0 + (k+1)\delta) + \int_{\tau_2}^{0} e^{-A_2(\xi)}\bar{g}_2(X_n)d\xi$$
$$\Rightarrow \|E(t)\| \le e^{\eta_2(1-n)\delta}(\eta_4 q_{\rm mod} + (1-n)\mu_2)\delta\|X_n(t)\| \quad (52)$$

where $0 \le \tau_2 < (1-n)\delta$. From (51) and (52), we obtain

$$\|E\| \le \beta_E\delta\|X_n\|$$
$$\beta_E = \max[e^{\eta_1 n\delta}(\eta_4 q_{\rm mod} + n\mu_1), e^{\eta_2(1-n)\delta}(\eta_4 q_{\rm mod} + (1-n)\mu_2)]. \quad (53)$$

Since $E = (X_n - X)$, we can use the result of Theorem 2 to show

$$\|X_n\| \le \beta_E\delta\|X_n\| + \|X\| \Rightarrow \|X_n\| \le \frac{\beta}{(1 - \beta_E\delta)} \quad (54)$$

where we assume $\delta < 1/\beta_E$.

REFERENCES

[1] M. Bodson and J. Chiasson, "A comparison of sensorless speed estimation methods for induction motor control.," in *Proc. Amer. Control Conf.*, Anchorage, AK, 2002, pp. 3076–3081.

[2] S. Carabelli and A. Tonoli, "System properties of flexible stuctures with self-sensing piezoelectric transducers.," *J. Sound Vib.*, vol. 235, no. l, pp. 1–23, 2000.

[3] F. R. Gantmacher, *The Theory of Matrices*. New York: Chelsea Publishing, 1959, vol. 1, pp. 239–241.

[4] J. P. Hespanha, "Root-mean-square gains of switched linear systems.," *IEEE Trans. Autom. Control*, vol. 48, no. 11, pp. 2040–2046, Nov. 2003.

[5] J. P. Hespanha and A. S. Morse, "Stability of switched systems with average dwell-time.," in *Proc. 38th Conf. Decision Control*, 1999, pp. 2655–2660.

[6] J. Holterman and T. J. A. de Vries, "Active and passive damping based on piezoelectric elements - controllability issues.," in *Proc. 3rd Workshop Eur. Sci. Ind. Collab.*, Enschede, The Netherlands, 2001, pp. 179–188.

[7] H. K. Khalil, *Nonlinear Systems.*, 3rd ed. Upper Saddle River, NJ: Prentice-Hall, 2002.

[8] T. Kim and M. Ehsani, "Sensorless control of the bide motors from, near-zero to high speeds.," *IEEE Trans. Power Electron.*, vol. 19, no. 6, pp. 1635–1645, 2004.

[9] D. Liberzon and A. S. Morse, "Basic problems in stability and design of switched systems.," *IEEE Control Syst. Mag.*, vol. 19, no. 5, pp. 59–70, Sep. 1999.

[10] S. O. Reza Moheimani, "A survey of recent innovations in vibration damping and control using shunted piezoelectric transducers.," *IEEE Trans. Control Syst. Technol.*, vol. ll, no. 4, pp. 482–494, Jul. 2003.

[11] S. S. Nudehi and R. Mukherjee, "Enhancing controllability and observability in underactuated and undersensed systems through switching: Application to vibration control.," *ASME J. Dynam. Syst., Meas., Control*, vol. 126, pp. 790–796, 2004.

[12] N. M. Thibeault and R. S. Smith, "Magnetic bearing measurement configurations and associated robustness and performance limitations.," *ASME J. Dynam. Syst., Meas., Control*, vol. 124, pp. 589–598, 2002.